Annals of Nuclear Medicine Vol. 10, No. 2, 225–230, 1996

Myocardial defect detected by ^{123}I-BMIPP scintigraphy and left ventricular dysfunction in patients with idiopathic dilated cardiomyopathy

Yasunori HASHIMOTO, Hiroshi YAMABE and Mitsuhiro YOKOYAMA

First Department of Internal Medicine, Kobe University School of Medicine

The present study examined the role of myocardial fatty acid in patients with idiopathic cardiomyopathy (DCM) by means of ^{123}I-β-methyl-p-iodophenyl pentadecanoic acid (^{123}I-BMIPP) scintigraphy. Thirteen patients underwent ^{123}I-BMIPP imaging, ^{201}Tl imaging and echocardiography. All patients showed defective myocardial uptake of ^{123}I-BMIPP and ^{201}Tl. The left ventricular end-diastolic dimension (64.1 ± 7.3 mm vs. 55.6 ± 1.5 mm, $p < 0.05$) and end-systolic dimension (52.4 ± 8.0 mm vs. 40.6 ± 2.1 mm, $p < 0.01$) were significantly larger in the large defect group (^{123}I-BMIPP defect score (DS) > 8) than the small defect group (DS < 7). The % fractional shortening (%FS) was also significantly smaller (18.6 ± 3.8% vs. 27.0 ± 3.3%, $p < 0.01$) in the large defect group. The ^{123}I-BMIPP DS correlated statistically with %FS ($r = 0.75$, $p < 0.01$), while the ^{201}Tl DS did not ($r = 0.41$, ns). We conclude that the patients with DCM revealed a ^{123}I-BMIPP uptake defect and the defect reflected the degree of left ventricular dysfunction.

Key words: DCM, ^{123}I-BMIPP, ^{201}Tl, echocardiography, left ventricular function

INTRODUCTION

IDIOPATHIC DILATED CARDIOMYOPATHY (DCM) is manifested by marked chamber dilation, diffusely reduced wall motion of the left ventricle and congestive heart failure; it has a poor prognosis. Although the pathogenesis of DCM has not been identified, previous myocarditis, microvascular dysfunction, toxins and myocardial metabolic disturbance have been suggested.[1] Calcium overload,[2,3] a decreased number of β-receptors[4] and inappropriate ventricular afterloading[5] are deterioration factors in ventricular dysfunction. Recent investigations have elucidated the disturbed myocardial metabolism of DCM including the involvement of glucose[6] and palmitate.[7] ^{123}I-β-methyl-p-iodophenyl pentadecanoic acid (^{123}I-BMIPP) is a new tracer used to assess myocardial fatty acid metabolism. ^{123}I-BMIPP is appropriate for use with single photon emission computed tomography (SPECT) because of its long-lasting accumulation in the myocardium and its high uptake ratio.[8–10] ^{123}I-BMIPP scintigraphy has provided fatty acid assessment in cardiomyopathic rats[11,12] and hypertensive rats[13] as well as in human hypertrophic cardiomyopathy.[14] Few studies have investigated DCM with ^{123}I-BMIPP scintigraphy. The present study was designed further to elucidate the characteristics of ^{123}I-BMIPP SPECT, and to investigate echocardiographic left ventricular dysfunction in patients with DCM using ^{123}I-BMIPP SPECT.

MATERIALS AND METHODS

Subjects: Thirteen patients with DCM (age 49 ± 16 years; ten males and three females) were selected for the study. The diagnosis of DCM was made by the criteria of the collaborative research project of the committees for Idiopathic Cardiomyopathy of the Ministry of Health and Welfare and of the Japanese Circulation Society. Ten of the patients had a history of congestive heart failure. The other three did not have a history of manifest congestive heart failure in spite of ventricular dysfunction. Twelve of the patients underwent coronary angiography, and none showed any coronary artery disease. A 38-year-old female patient did not undergo coronary angiography because she did not show any clinical signs of coronary

Received November 16, 1995, revision accepted February 23, 1996.

For reprint contact: Yasunori Hashimoto, M.D., First Department of Internal Medicine, Kobe University School of Medicine, 7–5–1, Kusunoki-cho, Chuo-ku, Kobe 650, JAPAN.

Table 1 Clinical manifestation of the studied subjects

Case No.	Age (years)	Sex	NYHA (class)	Echocardiogram					Scintigram	
				LVDd (mm)	LVDs (mm)	%FS (%)	IVS (mm)	PW (mm)	BMIPP DS	Tl DS
1	34	m	1	58	41	29	11	11	3	9
2	57	m	1	56	42	25	10	11	4	7
3	30	m	2	55	42	24	7	9	4	4
4	62	m	1	54	37	31	12	10	5	6
5	62	m	2	55	41	25	10	10	5	6
6	38	f	1	51	39	24	9	7	8	4
7	66	m	3	69	58	16	10	10	9	16
8	20	m	1	62	49	21	9	10	10	9
9	30	m	3	77	67	13	8	7	11	6
10	57	m	2	65	51	22	12	10	12	12
11	56	f	2	62	49	21	9	10	12	8
12	63	f	4	63	54	14	12	11	15	11
13	63	m	3	64	52	19	8	10	16	20
Mean	49.1		2	60.8	47.8	21.8	9.8	9.7	8.8	9.1
SD	16.1		1	7.1	8.6	5.5	1.6	1.3	4.3	4.7

NYHA: New York Heart Association, LVDd: left ventricular end-diastolic dimension, LVDs: left ventricular end-systolic dimension, %FS: % fractional shortening, IVS: thickness of interventricular septum, PW: thickness of posterior wall, LAD: left atrial dimension, DS: defect score

artery disease. Twelve patients had taken medication for heart failure; eleven patients had diuretics, nine had digitalis, four had angiotensin converting enzyme inhibitor and two had β-blocker. Informed consent to the ^{123}I-BMIPP scintigraphy was obtained from all patients.

SPECT imaging: All patients underwent both a ^{123}I-BMIPP scintigraphy and a ^{201}Tl scintigraphy under the resting condition. The average interval between the scintigraphies was 7 days, and their order was random. Patients fasted and discontinued medication 12 hours before each scintigraphy. 111 MBq of ^{123}I-BMIPP or 111 MBq of ^{201}Tl was injected intravenously, with the subject at rest in the upright position. The SPECT images were acquired 20 minutes after ^{123}I-BMIPP injection, and 5 minutes after ^{201}Tl injection in the supine position with a rotating gamma camera (ZLC75ECT, Siemens, German) and a computer analyzer (Scintipack 2400, Shimadzu, Japan). Both image sequences consisted of 32 projections with a 64 × 64 matrix acquired for 40 seconds (^{123}I-BMIPP) and 30 seconds (^{201}Tl) over a 180° circular orbit, from 60° left posterior oblique to 30° right anterior oblique. Contiguous transaxial tomographic images were obtained with a filtered back projection algorithm. Thereafter, long-axial, short-axial and horizontal-axial tomographic images were reconstructed from the transaxial tomographic images. In order to assess the myocardial uptake defects, we selected two short-axial slices (one each of the basal and apical part) and one long axial slice. Each short-axial slice was divided into 6 segments. The long-axis image was used for assessment of the apex. Thirteen segments were assessed in this way. The defects were graded visually on a scale of 0 to 2 (0: nearly normal, 1: mild to moderate, 2: severe). The grading was done by three skilled investigators. The total defect score (DS) was calculated as the summation of all the defect grades.

We then retrospectively divided the patients into two groups according to their DS from the ^{123}I-BMIPP image: the large defect group (DS > 8, n = 8) and the small defect group (DS < 7, n = 5). In addition, the defect pattern of the serial tomographic images was divided into two categories, i.e., a scattered patchy pattern of which the defect's size did not exceed a segment and a regional pattern of which the defect's size exceeded a segment.

Echocardiography: All patients underwent M-mode and two-dimensional echocardiography with an ultrasonoscope (SSH-140A, SSH-160A, Toshiba, Japan). The end-diastolic dimension (LVDd) and the end-systolic dimension (LVDs) of the left ventricle and percent fractional shortening (%FS) were measured with an M-mode strip chart averaging 5 sequential beats. The regional wall motion of the left ventricle was assessed visually with two-dimensional echocardiography. We compared the echocardiographic images and the scintigraphic image of each segment, and then examined the relationship between left ventricular wall motion and the myocardial defect of ^{123}I-BMIPP.

Statistical analysis: Values are expressed as the mean ± standard deviation. The comparison between the two groups was done by one-way analysis of variance test. A p value less than 0.05 was considered significant.

RESULTS

Patients' characteristics

Table 1 lists the clinical manifestations of the patients. Five patients were New York Heart Association (NYHA)

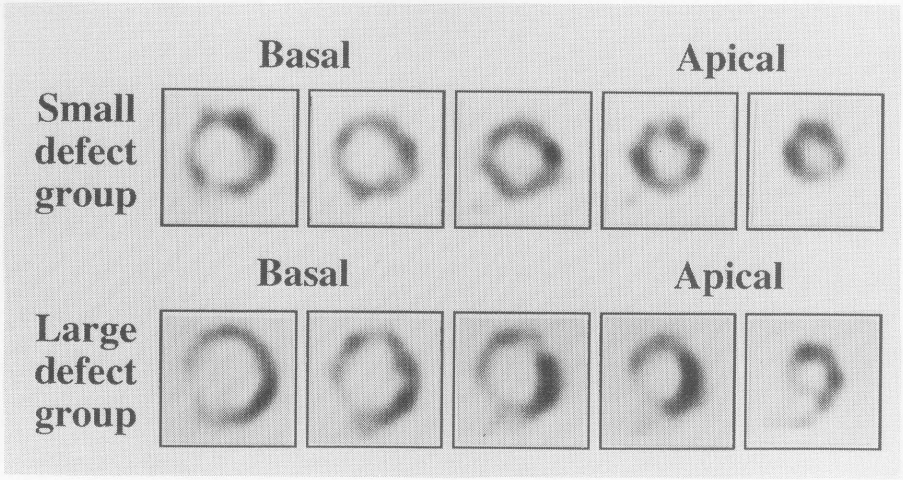

Fig. 1 The ^{123}I-BMIPP images of representative patients from the small defect group and the large defect group. The figures are serial short axial tomographies of ^{123}I-BMIPP images. The upper panel shows a case of small defect group with a patchy pattern, and the lower panel shows a case of large defect with a regional pattern.

class I, 4 patients were class II, 3 patients were class III, and one patient was class IV. Echocardiography revealed that all 13 patients had a dilated left ventricle and all except one had reduced %FS. Defects in myocardial ^{123}I-BMIPP uptake were found in all 13 patients. The DS of the ^{123}I-BMIPP image was 8.8 ± 4.3 (3 to 16). ^{201}Tl perfusion defects were also found in all patients. The DS of the ^{201}Tl image was 9.1 ± 4.7 (4 to 20). There was no significant difference between the DS obtained from the ^{123}I-BMIPP image and that from the ^{201}Tl image.

^{123}I-BMIPP imaging and ^{201}Tl imaging

Patients with the small defect group (n = 5) had a scattered patchy pattern. Patients with the large defect group (n = 8) had relatively large regional defects with or without patchy defects. The ^{123}I-BMIPP DS was 4.2 ± 0.8 in the small defect group and 11.6 ± 2.8 in the large defect group. The ^{201}Tl DS was 6.4 ± 1.8 in the small defect group and 10.8 ± 5.3 in the large defect group ($p < 0.001$). There was no difference between the small defect group and the large defect group in the patients' medication. Figure 1 shows representative cases. The upper panel shows the ^{123}I-BMIPP image of the small defect group and the lower panel shows that of the large defect group.

The location and size of the defects were compared in the ^{123}I-BMIPP images and ^{201}Tl images. The two images were consistent in 4 patients, but they were mismatced in 9 patients. Of these 9 patients, 4 cases showed a larger defect in the ^{123}I-BMIPP image than in the ^{201}Tl image; while 3 cases showed a smaller defect in the ^{123}I-BMIPP image than in the ^{201}Tl image, and in 2 cases defect locations were different. The consistent type was prevalent in the large defect group, but the mismatch type was less frequent in the small defect group.

Relationship between echocardiography and the scintigraphic images

Echocardiography revealed left ventricular dilation (LVDd ≥ 55 mm) and/or systolic dysfunction (%FS < 30%) in all patients except one and the abnormal wall motion in all patients. Advanced wall motion abnormality (akinesis or dyskinesis) was found in 8 patients. The ^{123}I-BMIPP image of 6 of these 8 patients showed defects in the akinetic or dyskinetic segments. Figure 2 shows the statistically significant differences between the large defect group and the small defect group in LVDd, LVDs and %FS. The LVDd (64.1 ± 7.3 mm vs. 55.6 ± 1.5 mm, $p < 0.05$) and LVDs (52.4 ± 8.0 mm vs. 40.6 ± 2.1 mm, $p < 0.01$) were larger in the large defect group than in the small defect group. The %FS was also smaller (18.6 ± 3.8% vs. 27.0 ± 3.3%, $p < 0.01$) in the large defect group. When patients were divided into two groups according the ^{201}Tl DS, there was no statistical difference in these echocardiographic findings (Table 2). Figure 3 shows that the ^{123}I-BMIPP DS correlated significantly with %FS ($r = 0.75$, $p < 0.01$), but the ^{201}Tl DS did not correlate with it ($r = 0.41$, ns).

DISCUSSION

The results of the present study indicate that the patients with DCM had a defective uptake of myocardial ^{123}I-BMIPP, and that the defect was related to left ventricular dysfunction.

^{123}I-BMIPP is a branched fatty acid. Most ^{123}I-BMIPP is trapped in the triglyceride fraction and a small percentage of ^{123}I-BMIPP is catabolized via β-oxidation in the cells.[8–10] The myocardial uptake of ^{123}I-BMIPP can be influenced by coronary flow, a decreased triglyceride pool, increased back diffusion from cells owing to re-

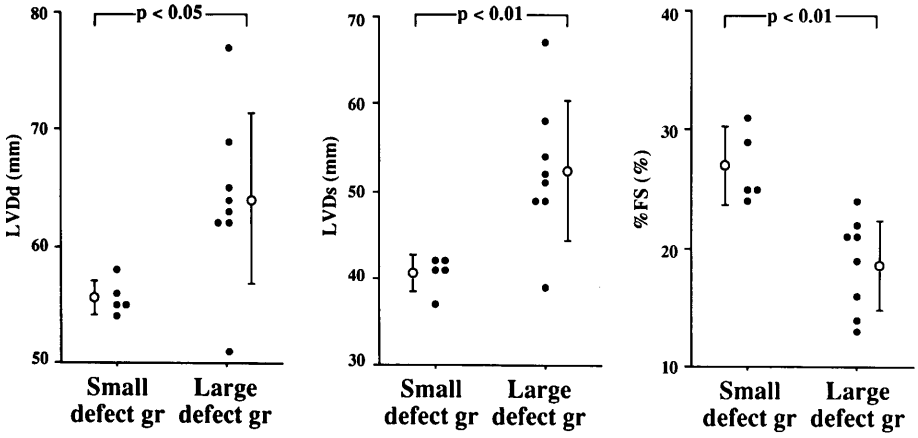

Fig. 2 Comparison of LVDd, LVDs and %FS in the small defect versus large defect groups. LVDd and LVDs were significantly larger and %FS was significantly smaller in the large defect group than in the small defect group (groups classified by defect score of ^{123}I-BMIPP SPECT).

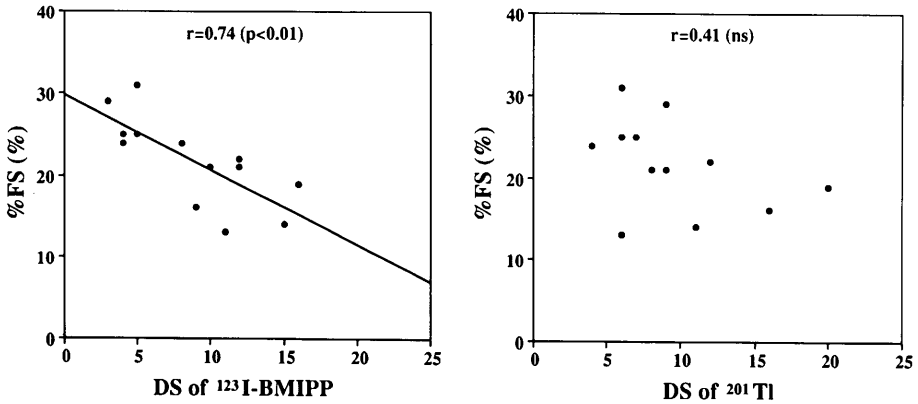

Fig. 3 The correlation between DS and %FS. The ^{123}I-BMIPP DS correlated significantly with %FS ($r = 0.75$, $p < 0.01$), and the ^{201}Tl DS did not ($r = 0.41$, ns).

Table 2 Echocardiography results

		n	DS	LVDd (mm)	LVDs (mm)	%FS (%)
BMIPP	Small defect group	5	4.2 ± 0.8	55.6 ± 1.5	40.6 ± 2.1	27.0 ± 3.3
	Large defect group	8	11.6 ± 2.8	64.1 ± 7.3*	52.4 ± 8.0**	18.6 ± 3.8**
Tl	Small defect group	6	5.5 ± 1.2	58.0 ± 9.5	44.7 ± 11.1	23.7 ± 6.0
	Large defect group	7	12.1 ± 4.4	63.3 ± 3.4	50.7 ± 5.3	20.3 ± 4.8

Abbreviations are the same as in Table 1. Small defect group: patient with DS ≤ 7, large defect group: patients with DS ≥ 8. *$p < 0.05$, **$p < 0.01$ (small defect group versus large defect group)

duced ATP, or the decreased myocardium itself. All of the patients in the present study had an abnormal ^{123}I-BMIPP image which was characterized by heterogeneity over the myocardium with patchy and/or regional lesions. This is consistent with the other studies with ^{11}C-palmitate.[7,15] These heterogeneous lesions of the myocardial metabolism may reflect the process of myocardial damage in DCM. The advanced wall motion abnormality corresponded with the defect in ^{123}I-BMIPP uptake. This accords with the report by Ugolini et al.[16] who used ^{123}I-phenylpentadecanoic acid which can be catabolized via β-oxidation. ^{123}I-BMIPP may therefore be valuable in the assessment of metabolic disorders in DCM, similar to the other tracers of physiological fatty acid.

Myocardial ischemia has been a main subject of past studies on myocardial fatty acid metabolism. ^{11}C-palmitate clearance, a function of fatty acid oxidation, deteriorated under ischemic and reperfused conditions.[17-19] The clearance correlates with the total amount of free fatty acid in the intercellular pool.[20,21] Since most ^{123}I-BMIPP is not rapidly catabolized in the mitochondria, our results do not directly indicate a decrease in the metabolic rate for fatty acid in DCM. It has been reported that the cellular ATP concentration correlates with ^{123}I-BMIPP uptake,[22]

and that mitochondrial damage caused by adriamycin correlates with ^{123}I-BMIPP uptake.[23] These reports suggest that ^{123}I-BMIPP uptake may reflect the state of energy production in the myocardium. The damage to myocardial cells in DCM may involve mitochondrial function, which decreases the oxidation of fatty acid. Reduced oxidative capacity can accelerate the depletion of the energy source for myocardial contraction. Impaired fatty acid metabolism may therefore be a cause as well as a result of myocardial dysfunction. This may be a reason why the ^{123}I-BMIPP uptake defect is related to left ventricular dysfunction.

The second important finding in the present study was mismatched defects between the ^{123}I-BMIPP image and the ^{201}Tl image. In 9 of the 13 patients, the defect revealed by the ^{123}I-BMIPP was not identical to the defect shown by the ^{201}Tl image. Such a mismatched defect is more frequent in the small defect group, and this suggests a less severe myocardial abnormality. In a study with a hamster model of DCM, the ^{123}I-BMIPP image showed a larger defect than did the ^{201}Tl image.[11,12] A study of spontaneously hypertensive rats reported that abnormal accumulation of ^{123}I-BMIPP developed faster than that of ^{201}Tl.[13] A ^{201}Tl defect indicates reduced coronary flow or myocardial mass. Since myocardial fibrosis develops into ventricular failure,[24] a ^{201}Tl image may indicate left ventricular dysfunction in DCM,[25–27] but the ^{201}Tl image in the present study did not accord with this concept. This may be related to the fact that the number of patients that we studied was small. There were 3 patients who had reverse mismatch of ^{123}I-BMIPP and ^{201}Tl defect, that is, the defect in the ^{201}Tl image was more predominant than the ^{123}I-BMIPP image. It is difficult to interpret the phenomenon of reverse mismatch. As we assessed the ^{123}I-BMIPP image by SPECT, diffusely reduced accumulation of ^{123}I-BMIPP as found in DCM may unmask a regional defect.

Clinical Implications: Left ventricular systolic dysfunction is a major feature of DCM. Echocardiographic or angiographic ventriculography, and the histological finding in biopsied ventricular specimens such as myocardial degeneration and fibrosis, have characterized the myocardial damage in DCM. The present study showed that ^{123}I-BMIPP scintigraphy provides new information on myocardial fatty acid metabolism which will be useful for the clinical assessment of patients with DCM, but the diagnostic value for prognosis and efficacy of treatment remains unclear.

CONCLUSION

SPECT with ^{123}I-BMIPP showed defective uptake of myocardial fatty acid in patients with DCM and the defects' relationship with left ventricular dysfunction.

REFERENCES

1. Unverferth DV. *Dilated Cardiomyopathy.* New York, Futura Publishing Company Inc., p. 213, 1985.
2. Gwathmev JK, Copelas L, MacKinnon R, Scoen FJ, Feldman MD, Morgan JP, et al. Abnormal intracellular calcium handling in myocardium from patients with end-stage heart failure. *Circ Res* 61: 70–76, 1987.
3. Movesian MA, Bristow MR, Krall J. Ca uptake by cardiac sarcoplasmic reticulum from patients with idiopathic dilated cardiomyopathy. *Circ Res* 65: 1141–1144, 1989.
4. Bristow MR, Ginsburg R, Minobe W, Cubicciotti RS, Sageman S, Stinson EB, et al. Decreased catecholamine sensitivity and beta-adrenergic receptor density in failing human hearts. *N Engl J Med* 307: 201–221, 1982.
5. Kurozumi H, Yokota Y, Inoh T, Fukuzaki H. Noninvasive estimation of myocardial damage in patients with dilated cardiomyopathy: Significance of afterload. *J Appl Cardiol* 5: 309–315, 1990.
6. Mody FV, Brunken RC, Stevenson LW, Nienaber CA, Phelps ME, Schelbert HR. Differentiating cardiomyopathy of coronary artery disease from nonischemic cardiomyopathy: Utilizing positron emission tomography. *J Am Coll Cardiol* 17: 73–383, 1991.
7. Geltman EM, Smith IL, Sobel BE, et al. Altered regional myocardial metabolism in congestive cardiomyopathy detected by positron tomography. *Am J of Med* 74: 773–785, 1983.
8. Knapp FF, Ambrose KR, Goodman MM. New Radioiodinated methyl-branched fatty acid for cardiac studies. *Eur J Nucl Med* 12: S39–S44, 1986.
9. Dudczak R, Scmoliner R, Knapp FF, Goodman MM. Structurally modified fatty acids: clinical potential as tracers of metabolism. *Eur J Nucl Med* 12: S45–S48, 1986.
10. Ambrose KR, Goodman MM, Knapp FF, et al. Evaluation of the metabolism in rat hearts of two new radioiodinated 3-methyl-branched fatty acid myocardial imaging agents. *Eur J Nucl Med* 12: 486–491, 1987.
11. Kurata C, Kobayashi A, Yamazaki N. Dual tracer autoradiographic study with thallium-201 and radioiodinated fatty acid in cardiomyopathic hamsters. *J Nucl Med* 30: 80–87, 1989.
12. Nishimura T, Sago M. Comparison of myocardial thallium and p-methyl iodophenyl pentadecanoic acid (BMIPP) distribution in cardiomyopathy hamster. *KAKU IGAKU (Jpn J Nucl Med)* 26: 897–900, 1989 (in Japanese).
13. Sago M, Nishimura T. Serial assessment of myocardial thallium perfusion and fatty acid utilization in spontaneously hypertensive rats: Assessment by autoradiography and pin-hole imaging. *KAKU IGAKU (Jpn J Nucl Med)* 26: 855–863, 1989 (in Japanese).
14. Kurata C, Tawarahara K, Aoshima S, Kobayashi A, Yamazaki N, Kaneko M, et al. Myocardial emission computed tomography with iodine-123-labeled beta-methyl-fatty acid in patients with hypertrophic cardiomyopathy. *J Nucl Med* 33: 6–13, 1992.
15. Eisenberg ID, Sobel BE, Geltman EM. Differentiation of ischemic from nonischemic cardiomyopathy with positron emission tomography. *Am J Cardiol* 59: 1410–1414, 1987.
16. Ugolini V, Hansen CL, Kulkarni PV, Jansen DE, Akers MS, Corbett JR, et al. Abnormal myocardial fatty acid metabo-

lism in dilated cardiomyopathy detected by iodine-123 phenylpentadecanoic acid and tomographic imaging. *Am J Cardiol* 62: 923–928, 1988.
17. Schelbert HR, Henze E, Keen R, Shon HR, Hansen H, Phelps ME, et al. ^{11}C-palmitate for the noninvasive evaluation of regional myocardial fatty acid metabolism with positron-computed tomography IV. *In vivo* evaluation of acute demand-induced ischemia in dogs. *Am Heart J* 106: 736–750, 1983.
18. Schwaiger M, Schelbert HR, Keen R, Johansen JV, Hansen H, Phelps ME, et al. Retention and clearance of ^{11}C-palmitic acid in ischemic and reperfused canine myocardium. *J Am Coll Cardiol* 6: 311–320, 1985.
19. Rosamund TL, Abendshein DR, Sobel BE, Bergman SR, Fox KAA. Metabolic rate of radiolabeled palmitate in ischemic canine myocardium: Implications for positron emission tomography. *J Nucl Med* 28: 1322–1329, 1987.
20. Schelbert HR, Henze E, Schon HR, Keen R, Hansen H, Phelps ME, et al. ^{11}C-palmitate for the noninvasive evaluation of regional myocardial fatty acid metabolism with positron computed tomography III. *In vivo* demonstration of the effects of substrate availability on myocardial metabolism. *Am Heart J* 105: 492–504, 1983.
21. Shon HR, Schelbert HR, Robinson G, Najafi A, Huang SC, Phelps ME, et al. ^{11}C-labeled palmitic acid for the noninvasive evaluation of regional myocardial fatty acid metabolism with positron computed tomography I. Kinetics of ^{11}C-palmitic acid in normal myocardium. *Am Heart J* 103: 532–547, 1982.
22. Fujibayashi Y, Yonekura Y, Takemura Y, Wada K, Matsumoto K, Yokoyama A, et al. Myocardial accumulation of iodinated beta-methyl-branched fatty acid analogue. Iodine-125-15-(p-iodophenyl)-3-(R.S)methylpentadecanoic acid (BMIPP) in relation to ATP concentration. *J Nucl Med* 31: 1818–1822, 1990.
23. Ogata M. Myocardial uptake of ^{123}I-BMIPP in rats treated with adriamycine. *KAKU IGAKU (Jpn J Nucl Med)* 26: 69–76, 1989 (in Japanese).
24. Kurozumi H, Yokota Y, Fukuzaki H. Clinical and histopathologic correlation in patients with dilated cardiomyopathy: Value of force-velocity product. *Jpn Heart J* 30: 431–441, 1989.
25. Burkey BH, Hutchins GM, Bailey I, Strauss HW, Pitt B. ^{201}Tl imaging and gated cardiac blood pool scans in patients with ischemic and idiopathic congestive cardiomyopathy. *Circulation* 55: 753–760, 1977.
26. Dunn RF, Uren RF, Sadick N, Sadick N, Bautovich G, Kelly DT, et al. Comparison of ^{201}Tl scanning in idiopathic dilated cardiomyopathy and severe coronary artery disease. *Circulation* 66: 804–810, 1982.
27. Tamai J, Nagata S, Nishimura T, Yutani C, Miyatake K, Nimura Y, et al. Hemodynamic and prognostic value of thallium-201 myocardial imaging in patients with dilated cardiomyopathy. *Int Jour of Cardiol* 24: 219–224, 1989.